Constitutive Modeling of the Cyclic Loading Response of Low Plasticity Fine-Grained Soils

Ross W. Boulanger(✉), Adam B. Price, and Katerina Ziotopoulou

University of California, Davis, CA 95616, USA

Abstract. Calibrations of the PM4Silt constitutive model are presented for two low-plasticity fine-grained soils that exhibit significantly different cyclic loading behaviors. The PM4Silt model is a stress-ratio controlled, critical state compatible, bounding surface plasticity model that was recently developed for representing low-plasticity silts and clays in geotechnical earthquake engineering applications. The low-plasticity clayey silt and silty clay examined herein were reconstituted mixtures of silica silt and kaolin with plasticity indices (PIs) of 6 and 20. Undrained monotonic and undrained cyclic direct simple shear (DSS) tests were performed on normally consolidated, slurry deposited specimens. Calibration of the PM4Silt model was based on the monotonic and cyclic DSS test data, plus empirical relationships for strain-dependent secant shear moduli and equivalent damping ratios. The calibration process and performance of the PM4Silt constitutive model are described for each soil. The results illustrate that PM4Silt is capable of reasonably approximating a range of monotonic and cyclic loading behaviors important to many earthquake engineering applications and is relatively easy to calibrate.

Keywords: Liquefaction · Cyclic softening · Silt · Constitutive model
Cyclic

1 Introduction

The selection of a constitutive model for representing liquefaction or cyclic softening of low-plasticity silts and clays in nonlinear dynamic analyses (NDAs) often requires considerable compromise in engineering practice. Low-plasticity silts and clays often exhibit cyclic loading behaviors that are intermediate to those exhibited by sand-like and clay-like soils, such that constitutive models developed for specifically for sands or clays may not reproduce the behaviors important to performance of systems with these types of intermediate low-plasticity fine-grained soils.

The PM4Silt plasticity model (Boulanger and Ziotopoulou 2018) was recently developed for representing low-plasticity silts and clays in geotechnical earthquake engineering applications. The PM4Silt model builds on the framework of the stress-ratio controlled, critical state compatible, bounding surface plasticity PM4Sand model (version 3) described in Boulanger and Ziotopoulou (2015) and Ziotopoulou and Boulanger (2016). Modifications to the constitutive relationships (relative to PM4Sand) were designed to improve the model's ability to approximate undrained monotonic and cyclic loading responses for low-plasticity silts and clays, as opposed to those for

A. Zhou et al. (Eds.): GSIC 2018, *Proceedings of GeoShanghai 2018 International Conference: Fundamentals of Soil Behaviours*, pp. 1–13, 2018.
https://doi.org/10.1007/978-981-13-0125-4_1

purely nonplastic silts or sands. The model was implemented as a dynamic link library for use with the finite difference program FLAC (Itasca 2016).

This paper presents calibrations of the PM4Silt model for two low-plasticity fine-grained soils that exhibit significantly different cyclic loading behaviors. The low-plasticity clayey silt and silty clay examined herein were reconstituted mixtures of silica silt and kaolin with plasticity indices (PIs) of 6 and 20. Undrained monotonic and undrained cyclic direct simple shear (DSS) tests were performed on normally consolidated, slurry deposited specimens. Calibration of the PM4Silt model was based on the monotonic and cyclic DSS test data, plus empirical relationships for strain-dependent secant shear moduli and equivalent damping ratios. The calibration process and performance of the PM4Silt constitutive model are described for each soil. The results illustrate that PM4Silt is capable of reasonably approximating a range of monotonic and cyclic loading behaviors important to many earthquake engineering applications and is relatively easy to calibrate.

2 PM4Silt Background

The PM4Silt model is a critical state and stress-ratio controlled bounding surface plasticity model developed for low-plasticity silts and clays that exhibit stress-history normalized undrained shear strengths. The bounding and dilation stress ratios are functions of the state parameter (ξ), such that they converge to the critical state stress ratio as the soil is shear to critical state ($\xi = 0$). The bounding surface relationship allows for separate adjustments for states that are loose or "wet" of critical state (i.e., $p' > p'_{cs}$ where p'_{cs} is the mean effective stress at critical state for the current void ratio) and dense or "dry" of critical state (i.e., $p' < p'_{cs}$), as illustrated in Fig. 1. The plastic modulus and dilatancy relationships are functions of fabric and fabric history terms. The model does not include a cap and therefore is not suited for simulating consolidation settlements under increasing overburden stresses or directly simulating strength evolution with consolidation stress history (e.g., along constant stress ratio loading paths). The constitutive equations and details of the model are provided in the manual by Boulanger and Ziotopoulou (2018).

The four primary input parameters are the undrained shear strength or undrained shear strength ratio at critical state $\left(s_{u,cs}/\sigma'_{vc}\right)$, shear modulus coefficient (G_o), contraction rate parameter (h_{po}), and post-strong-shaking shear strength reduction factor (F_{su}). The specified value for $s_{u,cs}$ is used internally to position the critical state line at the time of model initialization, conditional on the other input parameters, as illustrated in Fig. 2. The shear modulus coefficient should be selected to match the small-strain shear modulus (G_{max}) corresponding to the measured or estimated in-situ shear wave velocity. The contraction rate parameter should be calibrated to approximate the expected cyclic strength curve [i.e., cyclic resistance ratio (CRR) versus number of uniform loading cycles to reach a specified failure criterion]. The post-strong-shaking shear strength reduction factor is used in simulations of boundary value problems and is not applicable to the calibration examples presented herein; the value of F_{su} should

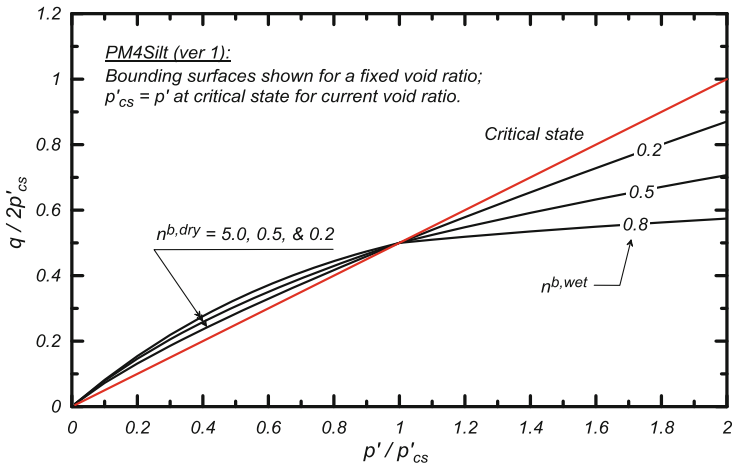

Fig. 1. Bounding surfaces on the wet and dry side of critical state for a constant void ratio.

be selected based on the soil characteristics and the shear strains that develop in the system during strong shaking as discussed in Boulanger and Ziotopoulou (2018).

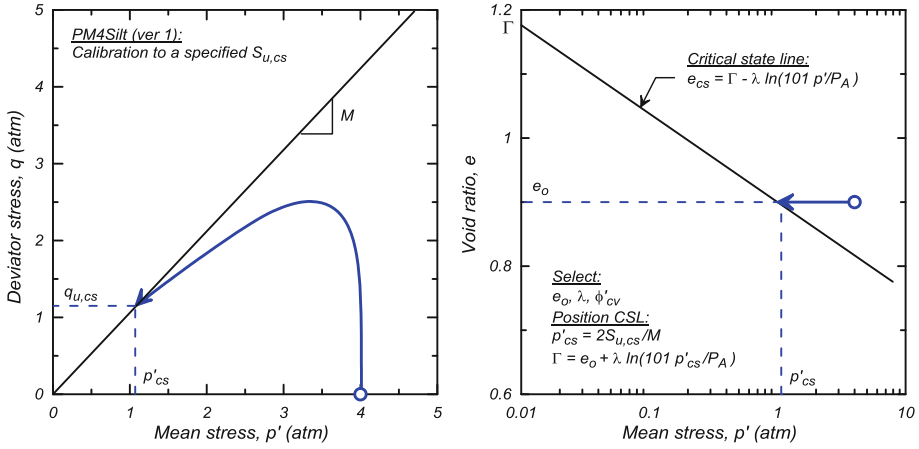

Fig. 2. Positioning the critical state line in PM4Silt based on the specified undrained shear strength and other input parameters.

The model has twenty secondary input parameters for which default values were developed based on a generalized calibration to typical cyclic loading behaviors. Default values are embedded in the initialization section of the model code and are applied unless specified otherwise by the user. Nonetheless, there are several parameters that the user may adjust for improved soil-specific calibrations, as illustrated in this paper.

The primary and secondary input parameters, along with their default values, are listed in Table 1. Responses of the model for a baseline set of primary input parameters in combination with the default secondary parameters are provided in the manual by Boulanger and Ziotopoulou (2018).

Table 1. Input parameters for PM4Silt.

Input parameter[a]	Default value	Calibrated values[c]	
		PI = 20 silty clay	PI = 6 clayey silt
$s_{u,cs}$ – s_u at critical state	–[b]	0.21	0.145
G_o – Shear modulus coefficient	–[b]	345	736
h_{po} – Contraction rate parameter	–[b]	1.2	2.2
n_G – Shear modulus exponent	0.75	1.0	–
h_o – Plastic modulus ratio	0.5	–	–
e_o – Initial void ratio	0.9	1.00	0.61
λ – Compressibility in e-ln (p') space	0.06	0.18	0.07
ϕ'_{cv} – Critical state friction angel	32°	25°	32°
$n^{b,wet}$ – Bounding surface parameter	0.8	1.0	–
$n^{b,dry}$ – Bounding surface parameter	0.5	–	–
n^d – Dilation surface parameter	0.3	–	–
A_{do} – Dilatancy parameter	0.8	–	–
$r_{u,max}$ – Sets bounding p_{min}	$p_{min} = p_{cs}/8$	–	0.99
z_{max} – Fabric term	$10 \leq 40\ (s_u/\sigma'_{vc}) \leq 20$	–	–
c_z – Fabric growth parameter	100	20	150
c_ε – Strain accumulation rate factor	$0.5 \leq (1.2\ s_{u,cs}/\sigma'_{vc} + 0.2) \leq 1.3$	0.25	1.0
C_{GD} – Modulus degradation factor	3.0	–	–
$C_{k\gamma f}$ – Plastic modulus factor	4.0	–	–
ν_0 – Poisson ratio	0.3	–	–

[a]Excluding post-shaking analysis parameters (F_{su}, PostShake, C_{GC}) and hour-glassing control parameters (cr_{hg}, c_{hg}).
[b]Required input parameter that does not have a default value.
[c]Retained default value if no entry listed.

3 Calibration of PM4Silt for a PI = 20 Silty Clay

The first soil examined herein is a normally consolidated, silty clay with a PI of 20, liquid limit (LL) of 42, and USCS classification of CL. This soil was manufactured by mixing 70% kaolin with 30% silica silt by dry mass. The silica silt was US Silica Sil-Co-Sil 250 from Ottawa, IL and the kaolin clay was Old Hickory Clay Company No. 1 Glaze from Hickory, KY. The mixture was hydrated as a slurry at twice its liquid limit, and then slurry deposited in the DSS mold for subsequent consolidation and testing. Test results are presented for specimens consolidated to an initial vertical effective stress $\left(\sigma'_{vc}\right)$ of 100 kPa. Monotonic and cyclic tests were generally performed at the same strain rate of 5%/h. Additional details regarding laboratory tests on these materials are provide in Price et al. (2015, 2017).

The process for calibrating PM4Silt is iterative, but the number of iterations can be minimized by sequencing the calibration steps in a logical order. There are a variety of sequences that can lead to an efficient calibration process, with the preferred sequence depending on the available information and the constitutive responses of primary interest. The process used for the present calibration can be summarized as follows:

[1] select values for the primary input parameters $s_{u,cs}$ (or $s_{u,cs}/\sigma'_{vc}$) and G_o,
[2] select values for any secondary parameters that can be informed by soil-specific test data, such as n_G, e_o, λ, and ϕ'_{cv},
[3] simulate the undrained monotonic DSS loading response and use $n^{b,wet}$ to adjust the peak s_u if the soil is initially wet of critical,
[4] simulate undrained cyclic DSS loading at different strain amplitudes and use h_o to adjust, as desired, the dependence of secant shear moduli and equivalent damping ratios on cyclic shear strain amplitude,
[5] simulate undrained cyclic DSS loading with uniform cyclic stress ratios and use h_{po} to adjust the fit to the cyclic DSS laboratory test data for CRR versus number of uniform loading cycles to cause a peak shear strain of 3%,
[6] examine the stress-strain and stress-path responses of the above cyclic loading simulations, and use other secondary parameters such as c_z, c_ε, and $r_{u,max}$ to adjust the shear strain accumulation rate and other features of behavior, and
[7] repeat steps [3] through [6] until no further revisions to input parameters are warranted.

The input parameters obtained by the above process for the PI = 20 silty clay are listed in Table 1. Per step [1], $s_{u,cs}/\sigma'_{vc}$ was set to 0.21 based on the monotonic DSS test results presented later and G_o was set to 345 based on the empirical correlation by Carlton and Pestana (2012). Per step [2], e_o was set to 1.0, λ to 0.18, and ϕ'_{cv} to 25° based on the responses of the DSS specimens during consolidation and shearing. Additional comments on the calibration process are provided with the following comparisons of simulated and measured or target responses.

Measured and simulated responses in monotonic undrained DSS loading are compared in Fig. 3. The simulated and measured shear strengths at critical state are the same, which reflects the fact that $s_{u,cs}$ is an input parameter. The parameter $n^{b,wet}$ was set to 1.0 because this limits the peak shear resistance to $s_{u,cs}$ in the simulation, which

matches the strain-hardening response observed in the test. The stress-strain response is initially much stiffer in the simulation than in the laboratory test, but this reflects the decision to base G_o and the target G/G_{max} behavior on empirical correlations, rather than attempting to match the measured DSS loading response. The stress-strain response measured in DSS tests is known to underestimate small strain stiffness due to various limitations with standard equipment, which means that adjusting G_o to match the measured DSS response would underestimate the true small-strain stiffness. The small-strain modulus and modulus reduction behavior are key concerns for any dynamic response analysis, so they were given priority in the calibration of the model parameters.

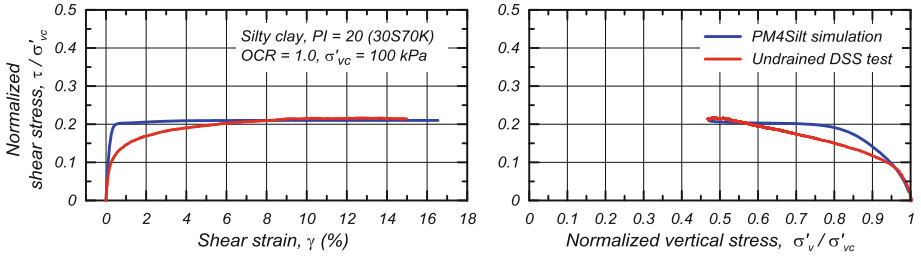

Fig. 3. Undrained monotonic DSS loading responses for the PI = 20 silty clay.

Normalized secant shear moduli (G/G_{max}) and equivalent damping ratios from simulations of undrained cyclic DSS loading at σ'_{vc} of 100 and 400 kPa are compared to the empirical curves by Vucetic and Dobry (1991) for PI = 0 and 15 soils in Fig. 4. The simulations have three cycles of loading at each strain amplitude; the secant shear modulus and damping ratio from the last cycle at each strain amplitude are the values plotted in Fig. 4. The G/G_{max} and equivalent damping ratios are close to the empirical PI = 15 curve for cyclic strain amplitudes less than about 0.03%, which was considered sufficiently reasonable to not warrant adjusting the parameter h_o. The more rapid drop in G/G_{max} and increase in damping ratios (relative to the empirical PI = 15 curves) as cyclic strain amplitudes exceed about 0.1% reflect cyclic degradation for this soft soil condition (e.g., stress-strain loops in the lower left plot of Fig. 4). This deviation from the empirical curves at larger strains is considered reasonable for this soft soil condition, and thus no attempt was made to improve the fit with the empirical curves at these larger strains. The simulations show a negligible effect of σ'_{vc} on G/G_{max} or equivalent damping ratios because the shear modulus exponent n_G was set equal to 1.0

Measured and simulated cyclic stress ratios (CSRs) required to cause a peak shear strain of 3% are plotted versus the number of uniform loading cycles in Fig. 5. The simulated cyclic strength will be approximately equal to the peak s_u/σ'_{vc} ratio near a single loading cycle. The parameter h_{po} was then iteratively adjusted to its final value of 1.2 to bring the simulated cyclic strength curve into an average agreement with the cyclic DSS test results.

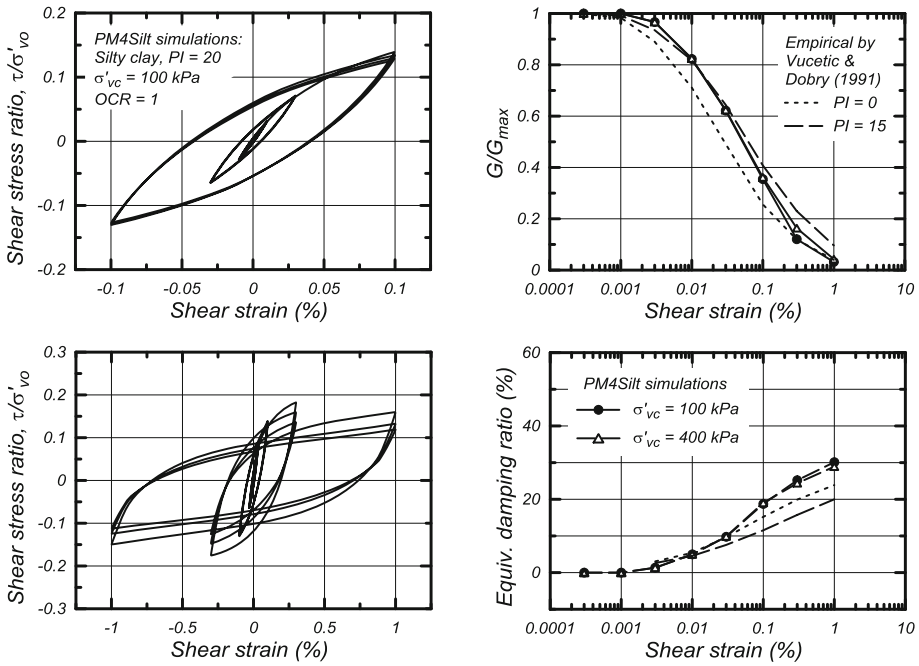

Fig. 4. Shear modulus and equivalent damping ratios from undrained cyclic loading at different shear strain amplitudes for the PI = 20 silty clay.

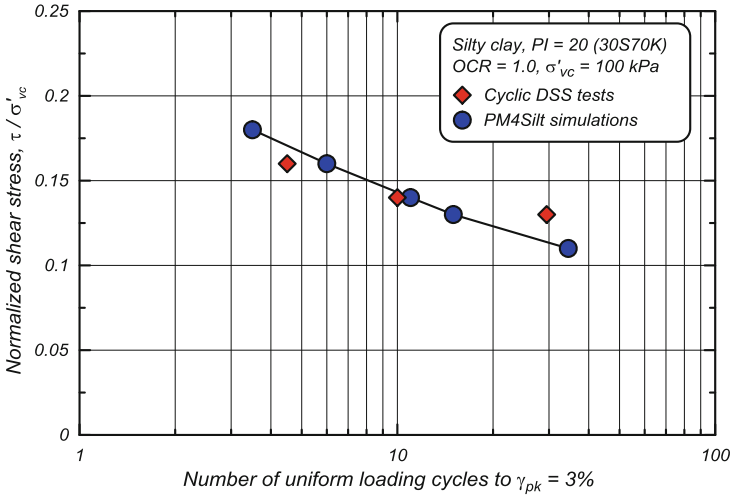

Fig. 5. Cyclic stress ratio versus number of uniform loading cycles to cause 3% shear strain in undrained cyclic DSS loading for the PI = 20 silty clay.

Measured and simulated stress-strain and stress-path responses are compared specimens loaded at CSRs of 0.16 and 0.13 in Figs. 6 and 7, respectively. The values for c_z and c_e were reduced to 20 (compared to a default value of 100) and 0.25 (compared to a default value of 0.5), respectively. These adjustments reduced the rates of shear strain accumulation in the simulations to levels consistent with the measured responses at different loading levels. The shear modulus exponent n_G was set to 1.0

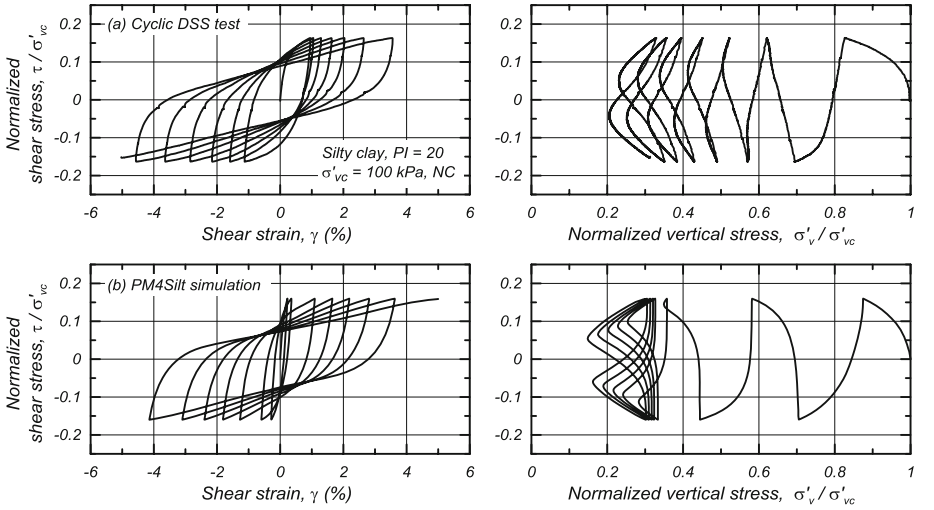

Fig. 6. Stress-strain and stress path responses in undrained cyclic DSS loading at a relatively high loading level for the PI = 20 silty clay.

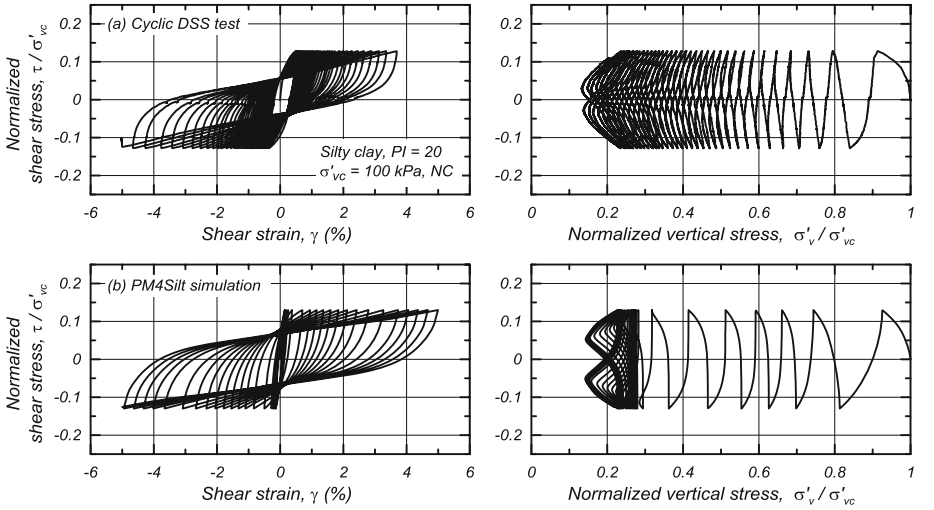

Fig. 7. Stress-strain and stress path responses in undrained cyclic DSS loading at a relatively low loading level for the PI = 20 silty clay.

because it slightly improved (narrowed) the stress-strain hysteresis loops and is consistent with other expectations for this more plastic fine-grained soil; e.g., minimal effects of σ'_{vc} on shear moduli and damping ratio values as shown in Fig. 4. The maximum excess pore pressure ratio was about 85–86% in the simulations (i.e., minimum σ'_v/σ'_{vc} of 0.14–0.15), which is in reasonable agreement with the measured values of 80–88%. The simulated stress-strain responses are in good agreement with the measured responses for both loading levels.

4 Calibration of PM4Silt for a PI = 6 Clayey Silt

The second soil examined is a normally consolidated, clayey silt with a PI of 6, LL of 22, and USCS classification of CL-ML. This soil was manufactured by mixing 20% kaolin with 80% silica silt by dry mass. The mixture was hydrated as a slurry at twice its liquid limit, and then slurry deposited in the DSS mold using the same general procedures as for the first soil. Test results are presented for specimens consolidated to an initial vertical effective stress (σ'_{vc}) of 100 kPa. Additional details are provided in Price et al. (2015, 2017).

The calibration process for this soil was the same as described in the previous section. The input parameters obtained for this PI = 6 clayey silt are listed in Table 1. Per step [1], $s_{u,cs}/\sigma'_{vc}$ was set to 0.145 based on the monotonic DSS test results presented later and G_o was set to 736 based on the empirical correlation by Carlton and Pestana (2012). Per step [2], e_o was set to 0.61, λ to 0.07, and ϕ'_{cv} to 32° based on the responses of the DSS specimens during consolidation and shearing. Additional comments on the calibration process are provided with the following comparisons of simulated and measured or target responses.

Measured and simulated responses in monotonic undrained DSS loading are compared in Fig. 8. The simulated and measured shear strengths at critical state are the same, which again reflects the fact that $s_{u,cs}$ is an input parameter. The parameter $n^{b,wet}$ was left at its default value of 0.8 because this produced a slight peak in the shear resistance, consistent with the response observed in the test. The stress-strain response is a bit stiffer in the simulation than in the test, which again reflects the decision to base G_o and the target G/G_{max} behavior on empirical correlations, rather than attempting to match the measured monotonic DSS loading response.

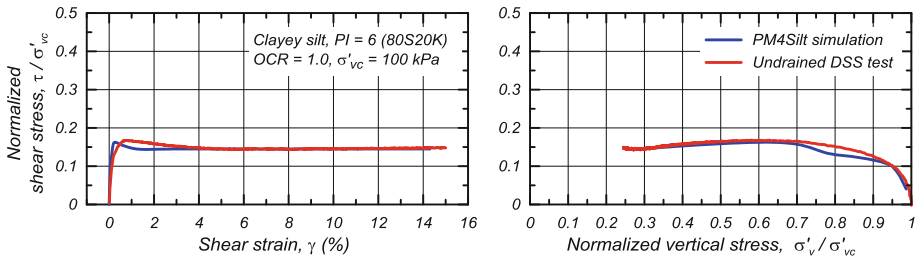

Fig. 8. Undrained monotonic DSS loading responses for the PI = 6 clayey silt.

Shear moduli and equivalent damping ratios from simulations of undrained cyclic DSS loading at σ'_{vc} of 100 and 400 kPa are compared to the empirical curves by Vucetic and Dobry (1991) for PI = 0 and 15 soils in Fig. 9. The shear moduli and equivalent damping ratios are close to the PI = 0 curve for cyclic strain amplitudes less than about 0.03%, which was considered sufficiently reasonable to not warrant adjusting the parameter h_o. The more rapid drop in shear moduli and increase in damping ratios as cyclic strain amplitudes exceed about 0.1% reflect cyclic degradation for this soft soil condition (e.g., stress-strain loops in the lower left plot of Fig. 9). This deviation from the empirical curves at larger strains is again considered reasonable for this soft soil condition. The simulations show a modest increase in G/G_{max} values and decrease in equivalent damping ratios with increasing σ'_{vc}, which is consistent with experimental trends. The simulations exhibit this stress dependence because the shear modulus exponent n_G was left at its default value of 0.75.

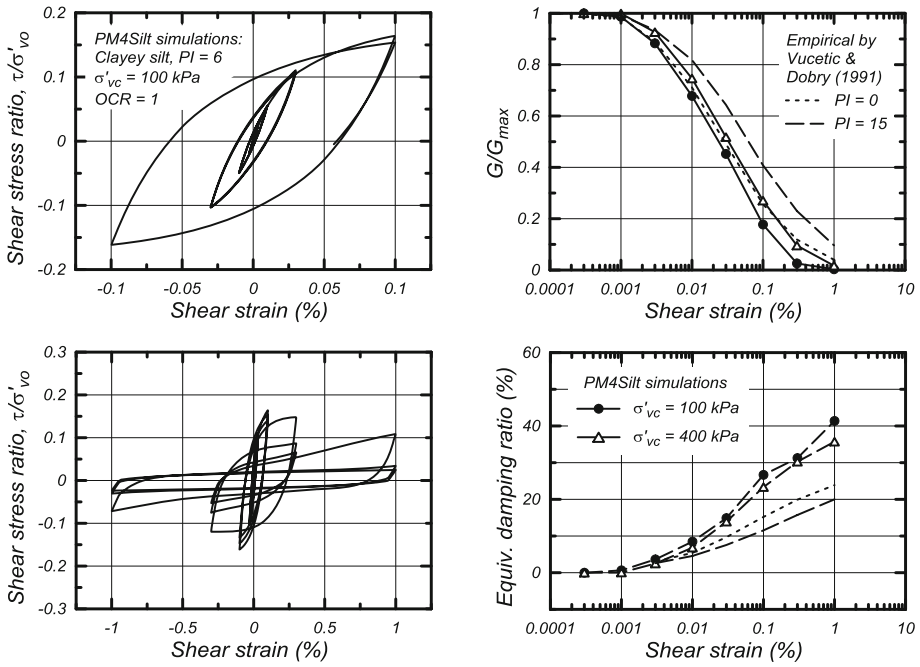

Fig. 9. Shear modulus and equivalent damping ratios from undrained cyclic loading at different shear strain amplitudes for the PI = 6 clayey silt.

Measured and simulated cyclic stress ratios (CSRs) required to cause a peak shear strain of 3% are plotted versus the number of uniform loading cycles in Fig. 10. The parameter h_{po} was iteratively adjusted to its final value of 2.2 to bring the simulated cyclic strength curve into average agreement with the cyclic DSS test results.

Measured and simulated stress-strain and stress-path responses are compared for specimens loaded at CSRs of 0.12 and 0.10 in Figs. 11 and 12, respectively.

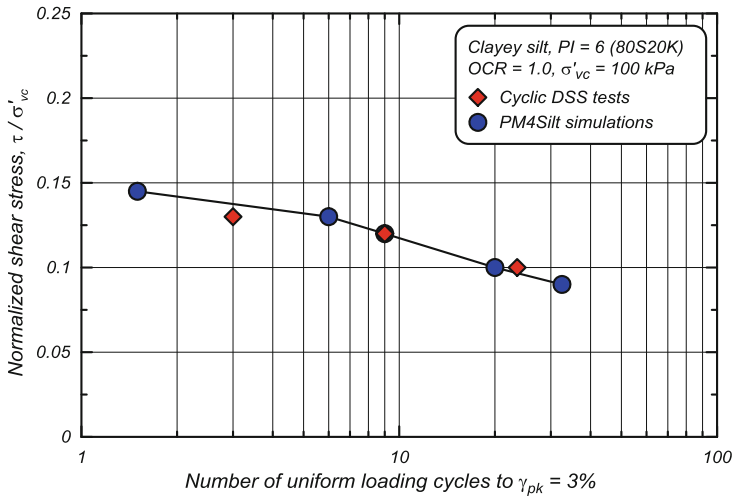

Fig. 10. Cyclic stress ratio versus number of uniform loading cycles to cause 3% shear strain in undrained cyclic DSS loading for the PI = 6 clayey silt.

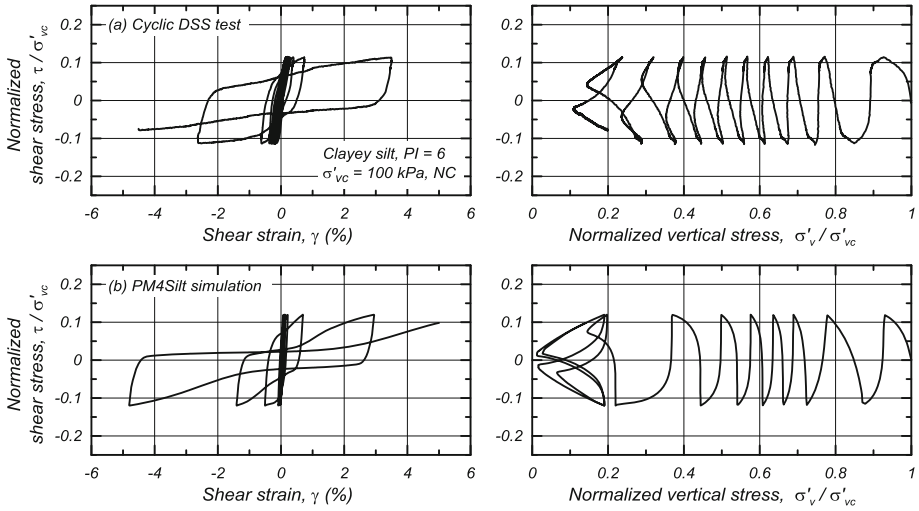

Fig. 11. Stress-strain and stress path responses in undrained cyclic DSS loading at a relatively high loading level for the PI = 6 clayey silt.

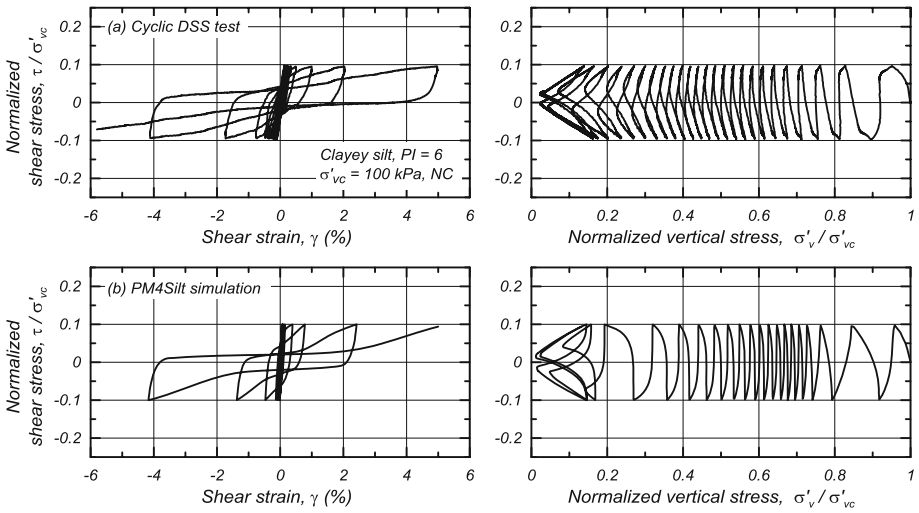

Fig. 12. Stress-strain and stress path responses in undrained cyclic DSS loading at a relatively low loading level for the PI = 6 clayey silt.

The parameter $r_{u,max}$ was set to 0.99 to enable the simulations to reach maximum excess pore pressure ratios consistent with those measured in the tests. The values for c_z and c_e were increased to 150 (compared to a default value of 100) and 1.0 (compared to a default value of 0.5), respectively. These adjustments increased the rates of shear strain accumulation in the simulations to levels consistent with the measured responses at different loading levels. The simulated stress-strain responses are in good agreement with the measured responses for both loading levels.

5 Concluding Remarks

Calibrations of the PM4Silt constitutive model recently developed by Boulanger and Ziotopoulou (2018) were presented for normally consolidated, slurry deposited specimens of a PI = 6 clayey silt and a PI = 20 silty clay. These two low-plasticity, fine-grained soils exhibited significantly different cyclic loading behaviors. The PI = 20 silty clay had greater monotonic and cyclic undrained shear strengths, and developed lower peak excess pore pressure ratios with slower rates of shear strain accumulation in cyclic undrained loading. The PM4Silt model was shown to be capable of reasonably approximating the monotonic and cyclic loading behaviors for both soils.

The calibration of PM4Silt or similar constitutive models for use in seismic analyses of geotechnical structures involves a number of considerations not discussed herein. For example, cyclic strengths obtained from conventional cyclic undrained DSS tests on high-quality field samples may require adjustments for strain-rate and multi-directional loading effects before being used to calibrate a constitutive model for use in a two-dimensional analysis. These and other aspects of constitutive model

calibration and evaluation practices are discussed in Boulanger and Beaty (2016) and Boulanger and Ziotopoulou (2018).

Acknowledgments. The work presented herein was derived from studies supported by the National Science Foundation (grants CMMI-1300518 and CMMI-1635398) and the California Department of Water Resources (DWR) under Contract 4600009751. Any opinions, findings, or recommendations expressed in this material are those of the authors and should not be interpreted as necessarily representing the official policies, either expressed or implied, of either organization.

References

Boulanger, R.W., Beaty, M.H.: Seismic deformation analyses of embankment dams: a reviewer's checklist. In: Proceedings, Celebrating the Value of Dams and Levees – Yesterday, Today and Tomorrow, 36th USSD Annual Meeting and Conference, United States Society on Dams, Denver, CO, pp. 535–546 (2016)

Boulanger, R.W., Ziotopoulou, K.: PM4Sand (Version 3): a sand plasticity model for earthquake engineering applications, 112 pp. Report No. UCD/CGM-15/01, Center for Geotechnical Modeling, Department of Civil and Environmental Engineering, University of California, Davis, CA (2015)

Boulanger, R.W., Ziotopoulou, K.: PM4Silt (Version 1): a silt plasticity model for earthquake engineering applications. Report No. UCD/CGM-18/01, Center for Geotechnical Modeling, Department of Civil and Environmental Engineering, University of California, Davis, CA (2018)

Boulanger, R.W., Ziotopoulou, K.: On NDA practices for evaluating liquefaction effects. In: Proceedings of Geotechnical Earthquake Engineering and Soil Dynamics V, ASCE Geo-Institute, Austin, TX, 10–13 June (2018, in press)

Carlton, B.D., Pestana, J.M.: Small strain shear modulus of high and low plasticity clays and silts. In: 15th World Conference on Earthquake Engineering, Lisbon, Portugal (2012)

Itasca: FLAC, Fast Lagrangian Analysis of Continua, User's Guide, Version 8.0. Itasca Consulting Group, Inc., Minneapolis, MN (2016)

Price, A.B., Boulanger, R.W., DeJong, J.T., Parra Bastidas, A.M., Moug, D.: Cyclic strengths and simulated CPT penetration resistances in intermediate soils. In: 6th International Conference on Earthquake Geotechnical Engineering, 14 November, Christchurch, New Zealand (2015)

Price, A.B., DeJong, J.T., Boulanger, R.W.: Cyclic loading response of silt with multiple loading events. J. Geotech. Geoenviron. Eng. **143**(10), 04017080 (2017). https://doi.org/10.1061/(ASCE)GT.1943-5606.0001759

Ziotopoulou, K., Boulanger, R.W.: Plasticity modeling of liquefaction effects under sloping ground and irregular cyclic loading conditions. Soil Dyn. Earthq. Eng. **84**, 269–283 (2016). https://doi.org/10.1016/j.soildyn.2016.02.013